Enhanced tunneling through nonstationary barriers

J. P. Palomares-Báez,[1] B. Ivlev,[2,3] and J. L. Rodríguez-López[1]
[1]*Advanced Materials Department, Instituto Potosino de Investigación Cientifica y Tecnológica, San Luis Potosí, San Luis Potosí 78231, Mexico*
[2]*Department of Physics and Astronomy and NanoCenter, University of South Carolina, Columbia, South Carolina 29208, USA*
[3]*Instituto de Física, Universidad Autónoma de San Luis Potosí, San Luis Potosí, San Luis Potosí 78000, Mexico*
(Received 8 January 2007; revised manuscript received 26 August 2007; published 7 November 2007)

Quantum tunneling through a nonstationary barrier is studied analytically and by a direct numerical solution of Schrödinger equation. Both methods are in agreement and say that the main features of the phenomenon can be described in terms of classical trajectories which are solutions of Newton's equation in complex time. The probability of tunneling is governed by analytical properties of a time-dependent perturbation and the classical trajectory in the plane of complex time. Some preliminary numerical calculations of Euclidean resonance (an easy penetration through a classical nonstationary barrier due to an underbarrier interference) are presented.

DOI: 10.1103/PhysRevA.76.052103 PACS number(s): 03.65.Xp, 03.65.Sq, 42.50.Hz

I. INTRODUCTION

The probability of quantum tunneling through a one-dimensional static potential barrier is described by the theory of Wentzel, Kramers, and Brillouin (WKB) [1] if the barrier is not very transparent. For a three-dimensional static barrier the semiclassical approach $\psi \sim \exp[iS(\vec{r})/\hbar]$ for the wave function is appropriate, where $S(\vec{r})$ is the classical action. The main contribution to the tunneling probability comes from the extreme path linking two classically allowed regions. The path can be parametrized as a classical trajectory in imaginary time $\vec{r}(i\tau)$; see, for example, Refs. [2–4]. The trajectory is a solution of Newton's equation in complex time. The wave function is well defined at each point of the trajectory.

For a nonstationary barrier one can also apply the method of classical trajectory in complex time [5–9]. But in contrast to the static case, this trajectory solely connects an initial and terminal physical points at a certain moment of time and does not track the whole underbarrier path as in the static case. One can say that the trajectory provides a semiclassical "bypass" of the complicated underbarrier dynamics through the plane of complex time [10–12]. This is the main difference in properties of trajectories for static and nonstationary barriers.

It follows that the underbarrier dynamics is governed by analytical properties of the nonstationary potential in the complex time plane. For example, a monochromatic ac field goes over into a large hyperbolic cosine [7–9] or a Lorentz shaped pulse is also amplified due to the pole structure in the plane of complex time [10–12].

The most delicate point of this theoretical construction is that the semiclassical approach for a wave function $\psi \sim \exp[iS(x,t)/\hbar]$, where $S(x,t)$ is an action for the nonstationary classic problem, is not valid at all times. Fast unavoidable processes break the semiclassical approach for short periods of time [10–14]. Since an exact analytical solution is absent, it is not completely clear how those processes may influence the semiclassical "bypass."

This problem becomes extremely important when we deal with Euclidean resonance (an easy penetration through a classical nonstationary barrier due to an underbarrier interference [11,12]). This process allows a description in terms of classical trajectories. The phenomenon of Euclidean resonance is surprising and counterintuitive since a particle emits quanta and tunnels with lower energy where, according to WKB, the barrier is less transparent. In this situation an evidence of applicability of the method of classical trajectories to nonstationary barriers would be valuable.

The goal of this paper is to show by numerical calculations the validity of semiclassical methods for the description of tunneling through a nonstationary potential barrier. The words "semiclassical methods" mean a possibility to approximate a wave function through the classical action $\psi \sim \exp[iS(x,t)/\hbar]$, excepting some short time intervals of a fast dynamics. In addition, this means there is a possibility to connect certain physical points by a classical trajectory which goes around the complicated dynamical regions, thus providing a "bypass" through the plane of complex time.

First, we consider in the paper photon-assisted tunneling which is a known phenomenon when an amplitude of the external nonstationary field is small and perturbation theory works. When the amplitude of the nonstationary field is not small the process becomes essentially multiquantum. The tunneling particle absorbs many quanta of the nonstationary field and exits from under the barrier with a higher energy. In this case perturbation theory is not applicable and one should use semiclassical methods, in particular, trajectories in complex time. It is shown in the paper that the main dynamical properties of photon-assisted tunneling are governed by analytical properties of classical trajectory in the plane of complex time.

Direct numerical solutions of the Schrödinger equation are obtained and compared with trajectory results. We check the threshold dynamics which follows from the main analytical properties of trajectories. A new branch of the wave function is only created when a position of a singularity of the external Lorentz shaped field in the plane of complex time is below compared to a singularity of the trajectory. The trajectory singularity relates to analytical properties of a solution of Newton's equation without an external nonstationary field [7–9]. We compared the numerically computed amplitude of

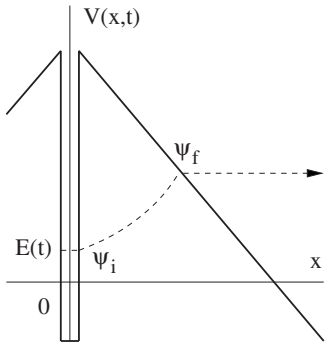

FIG. 1. The potential energy. $E(t)$ is a position of the discrete energy level in the δ well. The x axis is intersected at point $V/\mathcal{E}_0$. Tunneling, assisted by quanta absorption, occurs from the initial state ψ_i in the δ well to the final state ψ_f localized outside the barrier.

the output wave with the semiclassical one as a function of an amplitude of the nonstationary perturbation. All the numerical results are consistent with ones based on the trajectory method.

Second, we performed some preliminary numerical calculations of Euclidean resonance that corresponds to the opposite sign of the nonstationary perturbation. Euclidean resonance requires a more rigorous semiclassical condition compared to photon-assisted tunneling. This is due to the fact that a time interval Δt appears in the problem. This interval is not sufficiently long as can be seen in Sec. IX B. We shown that in our situation the proper semiclassical parameter, instead of being large, is of the order of unity. That parameter can be large enough for more thick potential barriers. At present, this is outside of possibilities of the numerical scheme used, so numerical studies of Euclidean resonance need further efforts.

Remarkable achievements in investigation of tunneling, including nonstationary barriers, are presented in Refs. [15–23].

II. FORMULATION OF THE PROBLEM

We consider tunneling through the one-dimensional nonstationary barrier

$$V(x,t) = V - \mathcal{E}_0|x| - \hbar\sqrt{2/m}\sqrt{V - E(t)}\,\delta(x), \tag{1}$$

shown in Fig. 1. The function $E(t)$ varies slowly compared to the time scale $\hbar/V$. For this reason, $E(t)$ can be treated as a discrete energy level in the δ well and plays a role of a nonstationary drive. We suppose the function $E(t)$ to be even and $E(t) < V$. When t is pure imaginary the energy $E(t)$ is real.

In papers [10–12] the δ function was static, but the outside potential was dynamical. In the present paper the situation is opposite. The outside static potential enables one to apply the reflectionless algorithm in the numerical calculations [24].

III. THE SEMICLASSICAL SOLUTION

Below we measure the coordinate in units of $V/\mathcal{E}_0$ and time in units of $\sqrt{2mV}/\mathcal{E}_0$. In these units the Schrödinger equation reads

$$\frac{i}{B}\frac{\partial\psi}{\partial t} = -\frac{1}{B^2}\frac{\partial^2\psi}{\partial x^2} + (1-x)\psi. \tag{2}$$

The δ function in the potential (1) is accounted for by the boundary condition

$$\left.\frac{\partial\psi(x,t)}{\partial x}\right|_{x=0} = -B\sqrt{1-h(t)}\,\psi(0,t), \tag{3}$$

where we introduce the dimensionless discrete level $h(t) = E(t)/V$ in the δ well and the large semiclassical parameter

$$B = \frac{V\sqrt{2mV}}{\hbar\mathcal{E}_0}. \tag{4}$$

The process is symmetric in x and we consider a positive x only. One can write the wave function in the form

$$\psi(x,t) = a(x,t)\exp[iS(x,t)], \tag{5}$$

where $S(x,t)$ is the classical action, measured in the units of Planck's constant $\hbar$ and satisfying the Hamilton-Jacobi equation [25]

$$\frac{1}{B}\frac{\partial S}{\partial t} + \frac{1}{B^2}\left(\frac{\partial S}{\partial x}\right)^2 + 1 - x = 0. \tag{6}$$

In the semiclassical limit, $1 \ll B$, the preexponential function $a(x,t)$ in Eq. (5) is less significant since it provides a soft x and t dependence compared to a strong dependence given by the exponent $\exp(iS)$. The semiclassical approximation of the wave function $\psi \sim \exp(iS)$ is called the exponential one. We use this approximation below.

The boundary condition for the action follows from Eq. (3),

$$\left.\frac{\partial S(x,t)}{\partial x}\right|_{x=0} = iB\sqrt{1-h(t)}. \tag{7}$$

In the static case, when $h(t)=0$, the exponentially small tunneling probability is given by the WKB expression $w \sim \exp(-A_{WKB})$ [1] where

$$A_{WKB} = \frac{4B}{3}. \tag{8}$$

One can solve Eq. (6) by the method of variation of a constant [25],

$$\frac{S(x,t)}{B} = i\int_0^x dy\sqrt{1-y-\varepsilon(x,t)} - t\varepsilon(x,t) + iA(\varepsilon), \tag{9}$$

where $A(\varepsilon)$ is the certain function to be determined. The condition of independence of the action on the variable constant, $\partial S/\partial\varepsilon = 0$, has the form

$$\frac{1}{2}\int_0^x \frac{dy}{\sqrt{1-y-\varepsilon(x,t)}} = \frac{\partial A(\varepsilon)}{\partial \varepsilon} + it. \tag{10}$$

Under this condition

$$\frac{\partial S(x,t)}{\partial x} = iB\sqrt{1-x-\varepsilon(x,t)}. \tag{11}$$

The boundary condition (7) is satisfied if we put $\varepsilon(0,t)=h(t)$, which determines the function $t(\varepsilon)$ since the function $h(t)$ is given. At $x=0$ the condition (10) $t=i\partial A(\varepsilon)/\partial\varepsilon$ determines, in the implicit form, the function $A(\varepsilon)$ since ε is a known function of t. By means of the function $\tau(\varepsilon)=-it(\varepsilon)$ the condition (10) reads

$$\frac{1}{2}\int_0^x \frac{dy}{\sqrt{1-y-\varepsilon}} = \tau(\varepsilon) + it. \tag{12}$$

In this equation one can consider τ as a variable and $\varepsilon=h(i\tau)$. It is easy to show that

$$x = (\tau + it)[2\sqrt{1-h(i\tau)} - \tau - it]. \tag{13}$$

Equation (13) determines the function $\tau(x,t)$. As follows from Eqs. (11) and (13),

$$i\frac{\partial S(x,t)}{\partial x} = B[\tau + it - \sqrt{1-h(i\tau)}]. \tag{14}$$

The action can be calculated from the equation

$$iS(x,t) = B\int_{-it}^{\tau} d\tau_1 \frac{\partial x}{\partial \tau_1}[\tau(x_1,t) + it - \sqrt{1-h(i\tau)}]. \tag{15}$$

After a short calculation we obtain

$$\frac{iS(x,t)}{B} = \frac{2}{3}[\sqrt{1-h(i\tau)} - \tau - it]^3 - \frac{2}{3}[1-h(i\tau)]^{3/2} - (\tau + it)h(i\tau) + \int_{-it}^{\tau} d\tau_1 h(i\tau_1). \tag{16}$$

Equation (16) provides the semiclassical solution of the problem if to insert the function $\tau(x,t)$ from Eq. (13).

IV. PHOTON-ASSISTED TUNNELING

We specify below a time dependence of the energy level in the δ well (1), $E(t)=Vh(t)$, in the Lorentz form

$$h(t) = \frac{h}{1+\Omega^2 t^2}, \tag{17}$$

where h and Ω are dimensionless parameters satisfying the conditions $0<h<1$ and $\Omega \sim 1$. The pulse (17) is soft compared to the short time scale $1/B$. The particle under the barrier absorbs quanta of the external nonstationary perturbation (17) and exits from under the barrier with a higher energy as shown in Fig. 1. This process is called photon-assisted tunneling. From Eq. (16) one can analyze dynamics of the wave function (5). At $t\to-\infty$ the barrier is static. In this case, as follows from Eq. (13), $1-x=(1-\tau)^2$. Equations (5) (without the preexponent) and (16) result in the known WKB expression

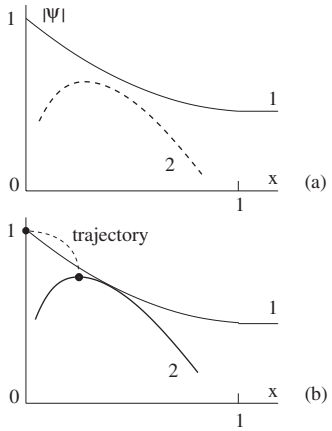

FIG. 2. The branches of the wave function at $0<h$ followed from the semiclassical approximation. (a) $t<0$. Curve 1 corresponds to the conventional WKB branch at $t\to-\infty$ when the barrier is static. Branch 2 still does not exist. (b) $t=0$. Branch 2 is created. The initial point (branch 1, $x=0$) and the final one (branch 2, the top point) are connected by the classical trajectory in imaginary time ("bypass"). x is measured in units of $V/\mathcal{E}_0$.

$$\psi \sim \exp\left(\frac{A_{WKB}}{2}[(1-x)^{3/2}-1]\right), \quad t\to-\infty. \tag{18}$$

Equation (18) relates to the branch indicated in Fig. 2(a) as 1.

In addition to that, as follows from Eq. (16), the new branch, denoted as 2 in Fig. 2(a), is near to being created. This means that, according to semiclassical approximation, it exists but the proper contribution to the wave function of the type (5) has zero coefficient $a=0$. When $h(t)$ reaches its maximum ($t=0$), the new branch touches branch 1, as in Fig. 2(b), and the coefficient a becomes nonzero. This short-time process is substantially nonsemiclassical. At positive t the new branch 2 moves away from the barrier as a semiclassical wave packet.

The states before and after tunneling are denoted as ψ_i and ψ_f in Fig. 1. The tunneling probability can be defined as $w=|\psi_f/\psi_i|^2$, where $\psi_i=\psi(0,0)$ is associated with the branch 1 and ψ_f is an amplitude value of branch 2 in Fig. 2(b). The tunneling probability, with the exponential accuracy, is given by

$$w \sim \exp[2iS(x_0,0)], \tag{19}$$

where x_0 relates to the maximum of the branch 2 where $\partial S(x,0)/\partial x=0$. It follows from Eqs. (13) and (14) that $x_0=\tau_0^2$. The parameter τ_0 satisfies the equation

$$1-\tau_0^2 = h(i\tau_0). \tag{20}$$

As follows from Eqs. (16) and (19),

$$w \sim \exp(-A), \quad A = 2B\left[\tau_0 - \frac{\tau_0^3}{3} - \int_0^{\tau_0} d\tau h(i\tau)\right]. \quad (21)$$

Equations (20) and (21) determine the tunneling probability with the exponential accuracy if to express τ_0 from Eq. (20) and to insert into Eq. (21).

In the static case, $h=0$, the particle escapes from under the barrier with zero energy. Under the nonstationary conditions the energy of the outgoing particle, δE, is determined by its potential energy $(1-x_0)V$ at the point x_0 since the kinetic energy is zero due to the condition $\partial S(x,0)/\partial x=0$ at that point. So the energy of the outgoing particle (the state ψ_f in Fig. 1) is

$$\delta E = (1 - \tau_0^2)V. \quad (22)$$

V. CLASSICAL TRAJECTORY

The tunneling probability is given, with the exponential accuracy, by Eqs. (20) and (21), which follow from the Hamilton-Jacobi formalism. In this section we show that the same result can be obtained by a simple method of classical trajectories in imaginary time $\tau=-it$. The classical trajectory starts at the top point of branch 2 in Fig. 2(b), where $\tau=0$ and $\partial x/\partial\tau=0$. The trajectory ends up at the certain imaginary time τ_0 where the coordinate $x(\tau_0)=0$ belongs to the δ well. This imaginary time τ_0 coincides with the parameter τ_0 introduced in Sec. IV. The trajectory is determined by Newton's equation

$$\frac{1}{2}\frac{\partial^2 x}{\partial \tau^2} = -1, \qquad \left.\frac{\partial x(\tau)}{\partial \tau}\right|_{\tau_0} = -2\sqrt{1 - h(i\tau_0)}. \quad (23)$$

The second equation is the boundary condition which coincides with Eq. (20). The solution has the form

$$x(\tau) = \tau_0^2 - \tau^2. \quad (24)$$

We consider the wave function not in the whole x,t plane but on the trajectory $\psi[x(\tau), i\tau]$. Then the equation holds

$$\psi[x(\tau_0), i\tau_0] = \exp\left(B\int_0^{\tau_0} d\tau\left[\frac{1}{4}\left(\frac{\partial x}{\partial \tau}\right)^2 + 1 - x\right]\right)\psi_f, \quad (25)$$

where $\psi_f = \psi[x(0),0]$ and the expression in the square brackets is the Lagrangian. Since the energy $E(t)=Vh(t)$ is a slow function of t the semiclassical relation

$$\psi[x(\tau_0), i\tau_0] = \exp\left[B\int_0^{\tau_0} h(i\tau)d\tau\right]\psi_i \quad (26)$$

is valid where $\psi_i = \psi[x(\tau_0),0]$. By means of Eqs. (25) and (26) one can write the tunneling probability $w=|\psi_f/\psi_i|^2$ in the form $w \sim \exp(-A)$, where

$$A = 2B\int_0^{\tau_0} d\tau\left[\frac{1}{4}\left(\frac{\partial x}{\partial \tau}\right)^2 + 1 - x - h(i\tau)\right]. \quad (27)$$

In this expression the parameter τ_0 is determined by Eq. (20). If we insert the solution (24) into Eq. (27), we obtain the previous result (21). The energy of the outgoing particle is given by the same expression (22) or, in other words, $\delta E = E(i\tau_0)$.

The trajectory in imaginary time provides a connection of the two points in Fig. 2(b) shown by the dashed curve. This is a "bypass" through the complex t plane of the complicated dynamics in real time. For our Lorentz pulse (17) it follows from Eqs. (20) and (21) that

$$\frac{A}{2B} = \tau_0 - \frac{\tau_0^3}{3} - \frac{h}{2\Omega}\ln\frac{1+\Omega\tau_0}{1-\Omega\tau_0}, \quad 1 - \tau_0^2 = \frac{h}{1-\Omega^2\tau_0^2}, \quad (28)$$

where one should choose a lowest root for τ_0. In the static case $(h=0)$ $\tau_0=1$ and A has the static limit value A_{WKB} (8).

When h is not zero the parameter Ω, indicating the width of the nonstationary pulse (17), plays a crucial role in the dynamics of the system. It is easy to show in the case of a small h. When $\Omega<1$ the parameter τ_0 hardly differs from unity, $\tau_0 = 1 - h/2(1-\Omega^2)$. Under this condition, A is close to its static limit value A_{WKB} and the energy of the outgoing particle $\delta E = hV/(1-\Omega^2)$ is small. The amplitude of the generated wave packet is close to the equilibrium value of the wave function $\exp(-A_{WKB}/2)$ at the conventional WKB exit point $x=1$. This means that the wave packet dynamics is not very pronounced.

When $1<\Omega$, due to the singularity of the pulse, even a small parameter h can substantially influence τ_0, which becomes approximately equal to $1/\Omega$ as follows from Eq. (28). As a result, one can present the action (28) at a small h in the form

$$A \simeq A_{WKB}\begin{cases} 1, & \Omega < 1, \\ (3\Omega^2 - 1)/2\Omega^3, & 1 < \Omega. \end{cases} \quad (29)$$

At $\Omega>1$ the outgoing particle has the energy $\delta E = (1-1/\Omega^2)V$.

We see that the tunneling rate is strongly increased (a reduction of A) when Ω exceeds the threshold value $\Omega=1$. This is a result of analytical properties of the function $h(t)$ in the complex plane which has a pole at $t=i/\Omega$. On the other hand, in the considered limit of a small h the classical trajectory has a singularity at $t=i$ which is simply a time of motion to the point $x=0$ of singularity of the potential (1) [7–9]. At $\Omega<1$ the pole of the external pulse is placed higher in the complex plane compared to the position of the trajectory singularity and the effect is weak. With the increase of Ω the two singularities merge at $\Omega=1$ and at a larger Ω the pole of $h(t)$ is beneath the trajectory singularity resulting in the strong effect.

One should note that the result (29) at $\Omega>1$ can be obtained by an approximate method of representation of the total probability as a product of one due to quanta absorption and another due to subsequent tunneling with a higher energy. An optimization with respect to the frequency of an individual quantum and a number of those absorbed quanta is generic, to some extent, with the trajectory method. We do not repeat the calculation here but refer the reader to Ref. [10].

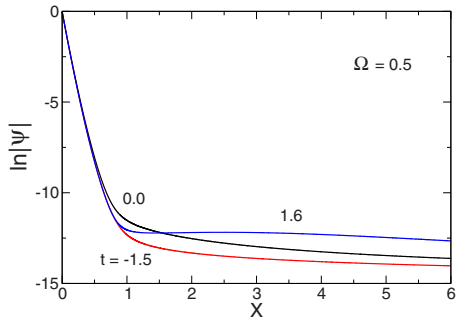

FIG. 3. (Color online) The numerically calculated dynamics of the wave function for $h=0.1$ and $B=20$ when Ω is less than the threshold. x is measured in units of $V/\mathcal{E}_0$.

VI. NUMERICAL STUDY OF PHOTON-ASSISTED TUNNELING

In order to check the above predictions we performed the direct numerical solution of the Schrödinger equation using the difference Crank-Nicolson scheme. The δ function was modeled by a deep rectangular well of the width of a few steps $\delta x=5\times10^{-4}$ in coordinate. We used different steps in time δt between 5×10^{-4} and 5×10^{-5} and different calculation precisions of 15, 30, and 100 digits. At the points $x=\pm6$ the transparent boundary conditions were imposed [24]. In order to match this reflectionless scheme the potential was chosen at a nonzero x in the form $(1-|x|)$ at $|x|<6$ and -5 otherwise. According to quantum mechanical calculations, the reflection due to the change of the potential slope at $x=6$ is small, of the order of 10^{-3} [1]. In the numerical calculations no reflection was observed. First, we calculated a wave function for a static potential $[h(t)=0]$. Then we switched on the pulse (17) and started with a large negative t when $h(t)$ was very small to exclude switch effects.

At sufficiently moderate $\Omega\leq1$ no formation of an outgoing packet was observed, as demonstrated in Fig. 3. The increase of the tunneling rate, due to a small reduction of the barrier slope, is small. This relates to the result (29) at $\Omega<1$.

At a larger $\Omega\geq1$ (Fig. 4) a very pronounced wave packet is formed which propagates away from the barrier. This relates to the result (29) at $\Omega>1$.

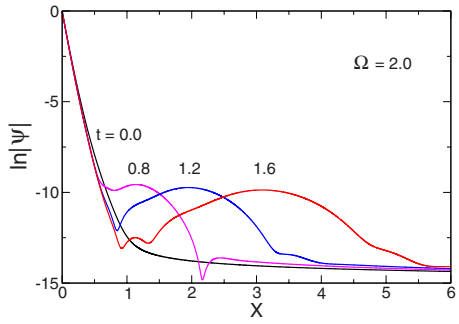

FIG. 4. (Color online) The numerically calculated dynamics of the wave function at $h=0.1$ and $B=20$ when Ω exceeds the threshold. x is measured in units of $V/\mathcal{E}_0$.

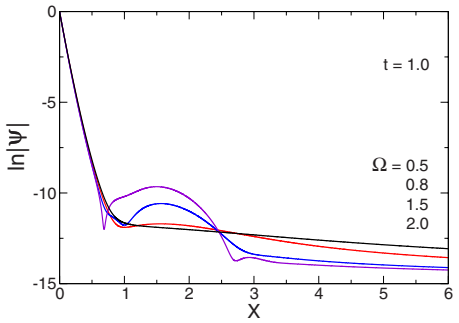

FIG. 5. (Color online) The numerically calculated wave function at $h=0.1$ and $B=20$. There is the crossover between the smooth behavior at $\Omega=0.5$ and 0.8 and the qualitatively different dynamics (wave packet formation) at $\Omega=1.5$ and $\Omega=2.0$. x is measured in units of $V/\mathcal{E}_0$.

The dynamics of the packet generation in Fig. 4 corresponds to the theoretical scenario sketched in Fig. 2. At $t=0$ the wave function hardly differs from the static one since the new branch is formed but remains hidden as in Fig. 2(b). At a positive t the new branch moves to the right, resulting in the appearance of the packet in Fig. 4 at $t\simeq0.8$. At a larger t the wave packet smoothly disappears at the point $x=6$ where the reflectionless condition is imposed [24].

Figures 3 and 4 relate to different regimes with respect to the threshold frequency $\Omega=1$. Actually, the threshold behavior (29) occurs in the limit of a small h. The value $h=0.1$ used is small but finite and the threshold form (29) smears out into a narrow crossover region around $\Omega=1$. This can be clearly seen in Fig. 5 where for $\Omega=0.5$ and 0.8 the dynamics is smooth, but for $\Omega=1.5$ and 2.0 it changes qualitatively exhibiting a formation of the pronounced wave packet.

To demonstrate a further coincidence between the trajectory predictions and the numerical results we plot an amplitude of the wave packet versus h at $\Omega=2.0$ in Fig. 6. The theoretical curve for the moment $t=0$ follows from Eq. (28) where we take $|\psi|_{max}=\exp(-A/2)$. In this expression a pre-exponential factor is neglected. The numerical results are taken at the moment $t=1.0$ since at $t=0$ the branch is hidden. One can see from Fig. 6 that the both dependences are in a

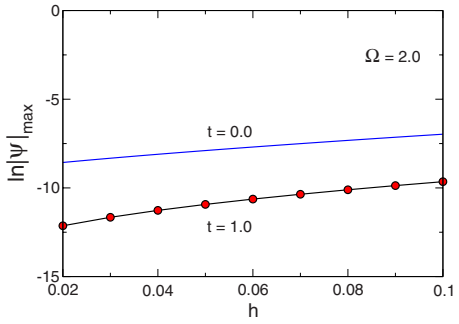

FIG. 6. (Color online) The numerically calculated dependence of the wave packet amplitude for $B=20$ at the moment $t=1.0$ versus h is shown by the circled curve. The theoretical dependence (without a pre-exponent) at $t=0$ is drawn by the solid curve. x is measured in units of $V/\mathcal{E}_0$.

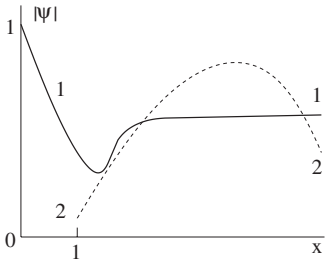

FIG. 7. The branches of the wave function at $h<0$ and the moment $t<-\Delta t$ followed from the semiclassical approximation. The initial branch 1-1 is deformed compared to the WKB state. The branch 2-2 almost touches branch 1-1 having a tendency to appear. x is measured in units of $V/\mathcal{E}_0$.

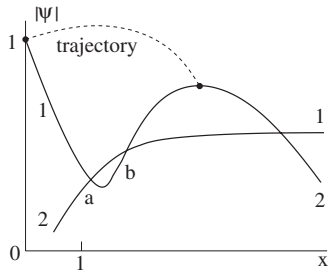

FIG. 8. The branches of the wave function at $h<0$ and the moment $t=0$ followed from the semiclassical approximation. The branches are already reconnected compared to Fig. 7. The classical trajectory in imaginary time (the dashed curve) connects the point at the potential well, $x=0$, and the top point. x is measured in units of $V/\mathcal{E}_0$.

reasonable agreement. The difference is due to a missing preexponential factor for the upper (theoretical) curve in Fig. 6. Another reason for the difference in the curves position is due to the fact that they are taken at different moments of time. The preexponential factor for branch 2 in Fig. 2(b) should be approximately 0.2 to obtain a coincidence.

One should note that when a position of the energy level in the δ well varies in time just within 2%, the semiclassical approach is still valid and the dynamics is governed by the analytical properties of $h(t)$ in the complex plane of time. The presented approach should be broken at sufficiently small h which is less than 0.02.

VII. EUCLIDEAN RESONANCE

In the previous sections we considered a positive particle energy $E(t)$ $(0<h)$, which results in a positive energy δE of the outgoing particle. In that case the energy of the state ψ_f in Fig. 1 is higher than the one for state ψ_i. This corresponds to photon-assisted tunneling.

When $E(t)$ is negative $(h<0)$ the exit energy δE can be negative when the energy of ψ_f is lower than the one for ψ_i. In this situation a phenomenon of Euclidean resonance can occur when quanta emissions strongly interfere with tunneling [11,12]. At negative h, the formalism, developed in Secs. III and V, remains valid if it is to formally change the sign of h. Analogously to Fig. 2, one can follow branch dynamics also at a negative h on the basis of Eqs. (13) and (16):

(1) At $t\to-\infty$, the situation is static and close to WKB.

(2) $t<-\Delta t$. Under increase of time the WKB branch 1-1 deforms as shown in Fig. 7. In addition to that, the branch 2-2, indicated in Fig. 7 and which still does not exist, has a tendency to appear. The parameter $\Delta t\sim 1$ can be evaluated from Eqs. (13) and (16).

(3) $t=-\Delta t$. The curve 2-2 touches the branch 1-1 and formation of the branch 2-2 occurs within the short nonsemiclassical time $1/B\ll 1$. Since the interval $\Delta t\sim 1$ is of a semiclassical order of magnitude, the fast nonsemiclassical processes, occurring within the time scale $1/B\ll 1$, have sufficient time to form the branch 2-2 in Fig. 8.

(4) $-\Delta t<t<\Delta t$. The reconnected branches are shown in Fig. 8 at $t=0$. Forms of them can be calculated by means of Eqs. (13) and (16) where one should substitute the function (17) with a negative h. There is a cubic algebraic equation for τ^2. One solution is real related to the branch 1-2 in Fig. 8. Two other complex conjugated solutions result in one branch of $|\psi|$. This is branch 2-1 in Fig. 8. It is remarkable that during this finite interval of time branch 1-2 starts at the potential well, $x=0$, and continues up to the point of maximum with no violation of semiclassical conditions. The maximum of branch 1-2 in Fig. 8 determines the tunneling probability given by Eqs. (20) and (21), which can also be calculated by a classical trajectory as in Sec. V. This trajectory is denoted in Fig. 8 by the dashed curve.

(5) $t=\Delta t$. The branches initially touch each other at some point and then they are detached during the short nonsemiclassical time $1/B\ll 1$.

(6) $\Delta t<t$. The generated branch 2-2 (similar to one in Fig. 7) is now physical and propagates to the right as a wave packet.

The formalism of classical trajectories in imaginary time, developed in Sec. V, results at $h<0$ in the tunneling probability

$$w\sim\exp(-A),\quad A=A_{WKB}f(\Omega,h)[\Omega-\Omega_R(h)],\qquad(30)$$

where the function $f(\Omega,h)$ is generally of the order of unity. At the resonance frequency $\Omega_R(h)$ the action formally equals zero. This phenomenon is called Euclidean resonance [11,12]. The approximation used allows one to approach the resonance frequency keeping the condition of small $\exp(-A)$. Otherwise, one has to use a multi-instanton formalism.

It is instructive to consider small $|h|\ll 1$ when one can easily obtain exact analytical formulas. We omit details since analogous calculations are demonstrated in Refs. [11,12]. In this case A has the form

$$A=A_{WKB}\frac{\sqrt{3}(1+\Omega\sqrt{3})}{2\Omega^3}[\Omega-\Omega_R(h)],\qquad(31)$$

with the resonance frequency

$$\Omega_R(h)\simeq\frac{1}{\sqrt{3}}\left(1-\frac{|h|}{4}\right).\qquad(32)$$

The energy of the outgoing particle (22) is

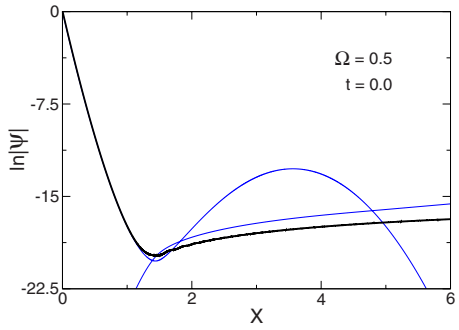

FIG. 9. (Color online) The case of $B=20$, $h=-0.28$, and $\Omega=0.5$ for the moment $t=0$. The thick curve shows the numerical result. The thin curves are analogous to the ones in Fig. 8 and are calculated from the semiclassical formalism of Sec. III (without a preexponent). x is measured in units of $V/\mathcal{E}_0$.

$$\delta E = \frac{\Omega^2 - 1}{\Omega^2} V. \tag{33}$$

Equations (31)–(33) are applicable for frequencies $\Omega_R < \Omega$. There is also an upper restriction for Ω. It should not exceed the semiclassical limit which, in the dimensionless units, is of the order of the large parameter A_{WKB}. In the physical units, this condition reads $\hbar\Omega \ll V$.

VIII. NUMERICAL STUDY OF EUCLIDEAN RESONANCE

For the case of a negative h the same numerical scheme is used as described in Sec. VI. We take the value $h=-0.28$. As follows from Eqs. (13) and (16), the resonance frequency in Eq. (30) is $\Omega_R(-0.28) \simeq 0.443$. For calculations the parameter $\Omega=0.5$ is taken. So, we are now a little away from the resonance. In other words, the maximum of branch 1-2 in Fig. 8 does not reach a value of the order of $|\psi(0,0)|$. By means of Eqs. (13) and (16) one can evaluate the important time interval discussed in Sec. VII as $\Delta t \simeq 0.22$.

The result of numerical calculations is shown in Fig. 9 by the thick curve that corresponds to the moment $t=0$. In the same figure the two branches, 1-2 and 2-1, of Fig. 8 are drawn as thin curves. Those branches are calculated on the basis of Eqs. (13) and (16), which account for only the classical action in Eq. (5) without the preexponent $a(x,t)$.

These numerical results are discussed in Sec. IX B.

IX. DISCUSSIONS

A. Photon-assisted tunneling

As one can see in Sec. VI, for photon-assisted tunneling $(0<h)$ the predictions made on the basis of the semiclassical theory are well confirmed by the numerical calculations. Namely, it is confirmed that a classical trajectory in complex time, defined by Newton's equation, plays a crucial role in underbarrier dynamics. Without a nonstationary drive such a trajectory has a singularity in the complex time plane which is determined by a form of the static potential barrier and a particle energy [7–9]. On the other hand, an external pulse of the Lorentz form in time has a pole at certain complex time. When this pole is lower in the complex plane than the trajectory singularity, the pronounced outgoing wave packet is formed.

Under the action of a smooth external drive the underbarrier dynamics is not semiclassical (smooth) at all times. At a certain moment there is a fast process of formation of a branch of the wave function. The classical trajectory in complex time provides a "bypass" of that complicated dynamics since along the complex trajectory the semiclassical approach is never violated.

One has to note that the semiclassical method, including classical trajectories, relates to a substantially multiquantum processes assisting tunneling when a nonstationary perturbation is not very small [10–12].

B. Euclidean resonance

For photon-assisted tunneling $(0<h)$ branch 2 in Fig. 2 is generated at the position of main branch 1. Therefore, during this process only a local in space redistribution of density occurs. In contrast to that, for Euclidean resonance $(h<0)$ the density redistribution should occur through a finite space interval. This is clear from Fig. 8 where the maximum of branch 1-2 is well away from the region close to $x=0$ from where the probability should come out.

The completely semiclassical solution, shown in Fig. 8, exists during the finite time $2\Delta t \sim 1$. The wave function from the region close to $x=0$ smoothly reaches the maximum along curve 1-2. Suppose this does not happen. In this case branch 1-2 in Fig. 8 intersects branch 2-1 at the points a and b and goes over into the same branch 2-1 at $x>b$. This nonsemiclassical abrupt cannot be smooth in time and is associated with an instability originated at region $a<x<b$. This instability implies a short time (of the order of $1/B \ll 1$) nonsemiclassical perturbations for which the time interval $\Delta t \sim 1$ is very long. The instability develops until the system reaches its semiclassical branches (Fig. 8), which are almost static compared to the instability time $1/B$. By means of the formalism of classical trajectories one can connect the two points in Fig. 8 providing a "bypass" of the complicated dynamics. So in the limit of large B one has to expect, within the time interval $-\Delta t < t < \Delta t$, the solution shown in Fig. 8.

Let us take a look at Fig. 9. There is a coincidence between the numerical curve and the theoretical ones. In order to obtain an exact coincidence one should shift the lower thin curve at the interval $2<x<6$ by $\ln|a|$ where $a \sim 0.4$ is the preexponential factor in Eq. (5). But part of branch 1-2 with the maximum is not generated. Why?

The time interval Δt of existence of semiclassical branches in Fig. 8, generally speaking, is of the order of unity. But for the parameters chosen $\Delta t \simeq 0.22$ is relatively short. This means that the two thin curves in Fig. 9 are not far from positions when they did touch each other at the moment $-\Delta t$ and when a did coincide with b. For $B=20$ one can estimate $B\Delta t \simeq 4.4$ that is not a sufficiently large number. In other words, during the interval Δt, which is short in our case, the nonsemiclassical instability does not have time to be developed. For photon-assisted tunneling $(0<h)$ the semiclassical parameter is B. For Euclidean resonance $(h$

<0) the analogous parameter, which also should be large, is $B\Delta t$. We see that the conditions of Euclidean resonance are more rigorous.

The interval Δt does not depend on B. If we take, say, $B=100$ (a very thick barrier), the parameter $B\Delta t \simeq 22$ is larger, which is more preferable for formation of the maximum in Fig. 9. Values of B larger than 40 bring essential problems into the numerical calculations. Fluctuations in the wave function close to $x=0$ should be small compared to the wave function at a large distance which is exponentially small as $\exp(-2B/3)$ or even less. Otherwise these fluctuations would transfer toward larger x and destroy a wave function at that region.

Another way to increase the parameter $B\Delta t$ is to take a larger $|h|$ in Eq. (5), keeping the same $B=20$. In this case the minimum of curve 1-2 in Figs. 8 and 9 becomes more deep. This requires a higher accuracy of calculations which is impossible for the numerical scheme used. For this reason, numerical studies of Euclidean resonance require further efforts.

X. CONCLUSIONS

The numerical solutions confirm the existing theoretical results that the main features of photon-assisted tunneling can be described by a classical trajectory in complex time. The probability of tunneling is governed by analytical properties of a nonstationary field and by those of a classical trajectory in the complex plane of time. This supports the general idea of applicability of trajectories to tunneling in a nonstationary case.

The results obtained open a way to apply the method of classical trajectories to more complicated problems of tunneling through nonstationary barriers, for example, to Euclidean resonance when the probability of tunneling through a classical barrier cannot be exponentially small. The preliminary numerical study of Euclidean resonance is presented in the paper. It is shown that Euclidean resonance occurs in more thick barriers compared to those allowed by the numerical scheme used.

ACKNOWLEDGMENTS

The authors (J.L.R.L. and J.P.P.B.) acknowledge support from CONACYT Grant No. J-42645F. J.P.P.B. acknowledges support from CONACYT.

[1] L. D. Landau and E. M. Lifshitz, *Quantum Mechanics* (Pergamon, New York, 1977).
[2] C. G. Callan and S. Coleman, Phys. Rev. D **16**, 1762 (1977).
[3] A. Schmid, Ann. Phys. **170**, 333 (1986).
[4] U. Eckern and A. Schmid, in *Quantum Tunneling in Condensed Media*, edited by A. Leggett and Yu. Kagan (North-Holland, Amsterdam, 1992).
[5] L. V. Keldysh, Zh. Eksp. Teor. Fiz. **47**, 1945 (1964) [Sov. Phys. JETP **20**, 1307 (1965)].
[6] V. S. Popov, V. P. Kuznetsov, and A. M. Perelomov, Zh. Eksp. Teor. Fiz. **53**, 331 (1967) [Sov. Phys. JETP **26**, 222 (1968)].
[7] B. I. Ivlev and V. I. Melnikov, Phys. Rev. Lett. **55**, 1614 (1985).
[8] B. I. Ivlev and V. I. Melnikov, Zh. Eksp. Teor. Fiz. **90**, 2208 (1986) [Sov. Phys. JETP **63**, 1295 (1986)].
[9] B. I. Ivlev and V. I. Melnikov, in *Quantum Tunneling in Condensed Media*, edited by A. Leggett and Yu. Kagan (North-Holland, Amsterdam, 1992).
[10] B. I. Ivlev, Phys. Rev. A **62**, 062102 (2000).
[11] B. I. Ivlev, Phys. Rev. A **66**, 012102 (2002).
[12] B. I. Ivlev, Phys. Rev. A **70**, 032110 (2004).
[13] B. Ivlev and V. Gudkov, Phys. Rev. C **69**, 037602 (2004).
[14] B. Ivlev, G. Pepe, R. Latempa, A. Barone, F. Barkov, J. Lisenfeld, and A. V. Ustinov, Phys. Rev. B **72**, 094507 (2005).
[15] S. Keshavamurthy and W. H. Miller, Chem. Phys. Lett. **218**, 189 (1994).
[16] T. Martin and G. Berman, Phys. Lett. A **196**, 65 (1994).
[17] A. Defendi and M. Roncadelli, J. Phys. A **28**, L515 (1995).
[18] N. T. Maitra and E. J. Heller, Phys. Rev. Lett. **78**, 3035 (1997).
[19] J. Ankerhold and H. Grabert, Europhys. Lett. **47**, 285 (1999).
[20] G. Cuniberti, A. Fechner, M. Sassetti, and B. Kramer, Europhys. Lett. **48**, 66 (1999).
[21] M. Saltzer and J. Ankerhold, Phys. Rev. A **68**, 042108 (2003).
[22] S. Zhang and E. Pollak, Phys. Rev. Lett. **91**, 190201 (2003).
[23] L. Hartman, I. Gouchuk, and P. Hänggi, J. Chem. Phys. **113**, 11159 (2000).
[24] M. Erhardt and A. Arnold, Riv. Mat. Univ. Parma **6/4**, 57 (2001).
[25] L. D. Landau and E. M. Lifshitz, *Mechanics* (Pergamon, New York, 1977).